

## Article

# Identification of Potential *Amblyomma americanum* Antigens After Vaccination with Tick Extracellular Vesicles in White-Tailed Deer

Adela Oliva Chávez <sup>1,2,\*</sup> , Julia Gonzalez <sup>1,†</sup> , Cristina Harvey <sup>1</sup>, Cárita de Souza Ribeiro-Silva <sup>3,‡</sup>, Brenda Leal-Galvan <sup>1,§</sup>, Kelly A. Persinger <sup>4</sup>, Sarah Durski <sup>2</sup>, Pia U. Olafson <sup>5</sup> and Tammi L. Johnson <sup>4</sup> 

- <sup>1</sup> Department of Entomology, Texas A&M University, College Station, TX 77843, USA; gonzalezj@exchange.tamu.edu (J.G.); harveycristina12@tamu.edu (C.H.); brenda.galvan@usda.gov (B.L.-G.)
- <sup>2</sup> Department of Entomology, University of Wisconsin-Madison, Madison, WI 73106, USA; sdurski@wisc.edu
- <sup>3</sup> Departamento de Biociências e Tecnologia, Instituto de Patologia Tropical e Saúde Pública, Universidade Federal de Goiás, Goiânia 74690-900, GO, Brazil; carsilva@koppert.com.br
- <sup>4</sup> Texas A&M AgriLife Research, Uvalde, TX 78801, USA; kelly.persinger@ag.tamu.edu (K.A.P.); tammi.johnson@ag.tamu.edu (T.L.J.)
- <sup>5</sup> United States Department of Agriculture—Agricultural Research Services (USDA-ARS), Knipling-Bushland United States Livestock Insects Research Laboratory, Kerrville, TX 78028, USA; pia.olafson@usda.gov
- \* Correspondence: olivachvez@wisc.edu; Tel.: +1-608-263-0834
- † Current address: Veterinary Integrative Biosciences, Texas A&M School of Veterinary Medicine & Biomedical Sciences, College Station, TX 77843, USA.
- ‡ Current address: Koppert Brazil Holding, Piracicaba 13420-280, SP, Brazil.
- § Current address: USDA-ARS Cattle Fever Tick Research Laboratory, Edinburg, TX 78541, USA.

**Abstract:** Background/Objective: Anti-tick vaccines represent a promising alternative to chemical acaricides for the management of ticks on wildlife; however, little progress has been made to produce a vaccine effective in wild hosts that are critical for tick reproduction, such as the white-tailed deer (*Odocoileus virginianus*). We recently tested *Amblyomma americanum* salivary and midgut extracellular vesicles as vaccine candidates in white-tailed deer, which resulted in on-host female tick mortality. The objective of this study was to identify the proteins recognized by the antibodies regenerated during these vaccinations to determine potential antigens for vaccine development for white-tailed deer. Methods: Using a proteomic approach, we characterized the cargo within salivary and midgut vesicles. Label-free quantitative proteomics were used to investigate significant changes in protein loading within extracellular vesicles in these two organs. The pre-vaccination and post-vaccination serum from three animals vaccinated with salivary and midgut vesicles and one control animal were used to identify proteins recognized by circulating antibodies. Results: We show that these salivary and midgut vesicles contain a “core-cargo” enriched in chaperones, small GTPases, and other proteins previously reported in small EVs. Label-free quantitative proteomics show significant differences in protein cargo between salivary and midgut vesicles (333 proteins out of 516). Proteomic analysis of immunoprecipitated proteins identified thirty antigens with potential for use in anti-tick vaccines, seven of which we have categorized as high priority. Conclusions: Proteins within tick salivary and midgut vesicles are recognized by antibodies from vaccinated white-tailed deer. These proteins can be further evaluated for their function and potential as vaccine candidates against ticks.

**Keywords:** tick vaccine; exosomes; microvesicles; proteomics; tick control; vaccine development



Academic Editors: Artur Sulik and Kacper Toczylowski

Received: 9 February 2025

Revised: 16 March 2025

Accepted: 19 March 2025

Published: 27 March 2025

**Citation:** Oliva Chávez, A.; Gonzalez, J.; Harvey, C.; Ribeiro-Silva, C.d.S.; Leal-Galvan, B.; Persinger, K.A.; Durski, S.; Olafson, P.U.; Johnson, T.L. Identification of Potential *Amblyomma americanum* Antigens After Vaccination with Tick Extracellular Vesicles in White-Tailed Deer. *Vaccines* **2025**, *13*, 355. <https://doi.org/10.3390/vaccines13040355>

**Copyright:** © 2025 by the authors. Licensee MDPI, Basel, Switzerland. This article is an open access article distributed under the terms and conditions of the Creative Commons Attribution (CC BY) license (<https://creativecommons.org/licenses/by/4.0/>).

## 1. Introduction

Ticks are important vectors of human and animal pathogens. In recent years, there has been a rise in the incidence of tick-borne diseases in the US [1]. Further, milder winters due to climate change will likely affect the geographic range of ticks, and, consequently, tick-borne diseases [2]. Among the tick species that most frequently bite humans in the US, *Amblyomma americanum* Linnaeus (Acari: Ixodidae; lone star tick) is known to transmit bacteria and viruses, and its bite may cause a delayed hypersensitivity to red meat in humans [3]. Additionally, this tick affects domestic animals, causing important economic damage and mortalities. For example, *A. americanum* infestations of cattle can result in weight loss in the absence of acaricide treatment [4]. This tick species is an aggressive biter that is expanding into the upper Midwest and northeast US [5] and it is predicted that increasing temperatures may permit expansion as far north as south Quebec, Canada [6,7]. Thus, management tools that will allow the control of this tick species on wildlife and domestic animals are desirable.

White-tailed deer (*Odocoileus virginianus* Zimmermann; WTD) are considered the most suitable host for *A. americanum* [8] and their presence within a landscape positively correlates with the abundance of several tick species, including *Ixodes ricinus* Linnaeus (Acari: Ixodidae) [9], *Ixodes scapularis* Say (Acari: Ixodidae) [10], and *A. americanum* [11]. Deer densities also correlate with the incidence of *A. americanum*-borne diseases [12] and they serve as reservoirs for the human pathogens *Ehrlichia chaffeensis*, the causative agent of human monocytic ehrlichiosis [13], and *E. ewingii* [14], a bacterium that infects neutrophils also causing human ehrlichiosis [15]. Given the importance of WTD in the density of several tick species and the transmission of tick-borne pathogens, interest in the development of management tools, including anti-tick vaccines, has grown [16]. Current studies treating WTD with permethrin using four-poster devices showed a significant decrease in host-seeking larvae, nymphs, and adults. Moreover, these treatments resulted in a reduction in *Ehrlichia* spp.-infected *A. americanum* [17]. However, four-poster devices present several complications, including their limited effectiveness at a broader geographic scale, difficulties with regulations in their proximity to residential areas, high operational costs, the banning of baiting in several states throughout of the US due to chronic wasting disease (CWD), withdraw periods due to meat consumption, and limited adoption by the public [18]. According to a study conducted in Connecticut and New York, only 37% of residents would support the placement of four-post devices within their properties, mostly due to safety concerns [19], thus, hindering their implementation. Although resistance to acaricides has not been reported in *A. americanum* populations, reports demonstrated potential development of tolerance against permethrins in wild *A. americanum* populations recovered from farmed and wild WTD [20]. Therefore, including immunological approaches (i.e., anti-tick vaccines) into integrated tick management programs is desirable [21]. Nevertheless, there are no current vaccines targeting *A. americanum* on WTD.

We recently tested the efficacy of tick salivary (SG) and midgut (MG) extracellular vesicles (EVs) as vaccine candidates in WTD, showing strong serum conversion [22]. Extracellular vesicles are small lipid-rich blebs that are secreted within tick saliva and hemolymph [23–25]. These vesicles are essential for tick feeding, pathogen transmission, and pathogen acquisition [24,26]. Interestingly, vaccinations with SG- and MG-EVs resulted in long-lasting circulating antibodies that were detected as far as 13 months after the last booster injection and led to 50.3% control due to on-host mortality of *A. americanum* females during feeding [22]. However, the antigens that elicited these immune responses remain to be identified. The objective of this study was to characterize the proteins that elicited an immune response within the vaccinated animals in our previous experiments.

## 2. Materials and Methods

### 2.1. Label-Free Quantitative Proteomic Analysis

Salivary (SG) and midgut extracellular vesicles used to vaccinate WTD were isolated from ex vivo organ cultures from *A. americanum* females fed for 5 days on WTD as previously described [22]. Three aliquots of 365  $\mu$ L of SG- or MG-EVs resuspended in 1X phosphate-buffered saline (PBS) were submitted to the Gehrke Proteomics Center at the University of Missouri for label-free quantitative proteomic analysis. Samples were processed as follows.

#### 2.1.1. Sample Preparation

Protein pellets were washed with 80% acetone in water and centrifuged at  $16,000\times g$  for 5 min. Pellets were suspended in 10  $\mu$ L urea buffer (6 M urea, 2 M thiourea, 100 mM ammonium bicarbonate, pH 8.0). Protein was digested at 37 °C overnight with 0.3  $\mu$ g trypsin. A second digestion was performed the next day with 0.2  $\mu$ g trypsin for 3 h. Peptides were desalted using 100  $\mu$ L Pierce C18 tips (ThermoFisher Scientific, Waltham, MA, USA, #87784). Lyophilized peptides were resuspended in 10  $\mu$ L 5% acetonitrile and 0.1% formic acid. Peptide concentration was determined using a Pierce Quantitative Colorimetric Peptide assay (Thermo Fisher Scientific, Waltham, MA, USA, #23275) and an equal amount of peptides were transferred into autosampler vials. The auto-sampler was cooled to 7 °C during the run.

#### 2.1.2. Mass Spectrometry

Peptides were analyzed by mass spectrometry, using the following procedure: 1  $\mu$ L injection was made onto a 20 cm long  $\times$  75  $\mu$ m inner diameter pulled-needle fused-silica analytical column packed with Waters BEH-C18, 1.7  $\mu$ m reversed-phase resin. Peptides were separated and eluted from the analytical column with a gradient of acetonitrile at 300  $\eta$ L/min. Liquid chromatography (LC) gradient conditions were as follows: initial conditions were 3% B (A: 0.1% formic acid in water, B: 99.9% acetonitrile, 0.1% formic acid), followed by a 10 min gradient to 17% B. Then 17–25% B over 20 min, 25–37% B over 10 min, 37–80% B over 6 min, ending with 3 flushing cycles (80% B–40% B for 2 min) and finally back to initial conditions (3% B) for 2 min and held for 4 min to equilibrate the column. Total run time was 60 min. Data were acquired on a timsTOF-PRO mass spectrometer (Bruker, Billerica, MA, USA).

Mass spectrometry (MS) data were collected in positive-ion data-dependent acquisition (DDA) parallel accumulation–serial fragmentation (PASEF) mode over an  $m/z$  range of 100 to 1700. PASEF and trapped ion mobility spectrometry (TIMS) were set to “on”. One MS and ten PASEF frames were acquired per cycle of 1.17 s. Target MS intensity for MS was set at 10,000 with a minimum threshold of 2500. A charge-state-based rolling collision energy table from 20–59 eV was used. An active exclusion/reconsider precursor method with release after 0.4 min was used. If the precursor (within mass width error of 0.015  $m/z$ ) was  $>4\times$  signal intensity in subsequent scans, a second MS/MS spectrum was collected. Isolation width was set to 2 ( $<700 m/z$ ) or 3 (800–1500  $m/z$ ).

#### 2.1.3. Data Analysis

The DDA-PASEF individual runs were analyzed with Fragpipe version 18.0 using the “Label free quantification (LFQ)- match between runs (MBR)” workflow, which included the database search against Uniprot *Ixodes scapularis* (20,486 entities) with MSFragger version 3.5. This database enabled us to perform enrichment analyses based on the annotated *I. scapularis* genome. Although an annotated genome is available for *A. americanum* through National Center for Biotechnology Information (NCBI) (GCA\_030143305.2), its proteins

are not accessible through Panther [27]. Philosopher version 4.4.0 was used for peptide–spectrum match (PSM) validation and protein inference and IonQuant for MS1-level label-free quantification. For MS1-level quantification, the MBR and normalization were enabled along with the MaxLFQ algorithm, and a minimum number of 2 ions was required for quantifying a protein in IonQuant. For feature detection in IonQuant, 10 ppm, 0.4 min, and 0.05 1/k0 were set for  $m/z$ , retention time, and ion mobility tolerances, respectively.

Data were searched with trypsin as the digestive enzyme, two missed cleavages were allowed, carbamidomethyl cysteine was included as a fixed modification, and oxidized methionine and N-terminal acetylation were used as variable modifications. The mass tolerances were set at 20 ppm for precursor ions and 0.1 Da for fragment ions. Data were exported and further analyzed with Perseus version 1.6.5.0. Only proteins with at least one unique peptide/protein and four total spectral of each whole set were used for quantitative comparison. Significant differences in quantification were evaluated by Student's *t*-test followed by Benjamini Hochberg correction.

## 2.2. Extracellular Vesicle Cargo Comparison and Pathway Enrichment Analysis

Proteomic data were exported into Excel spreadsheets for analysis. Normalized intensity counts of the spectra (Supplementary File S1) were used to identify the cargo within each EV type. The UniProt ID from proteins with spectra counts in all three biological replicates and technical duplicates were filtered and the SG- and MG-EV cargo were compared using <https://molbiotools.com/listcompare.php> (accessed on 11 November 2024) to identify shared and unique proteins.

UniProt IDs of proteins shared between SG- and MG-EVs (Supplementary File S2), proteins unique to SG-EVs (Supplementary File S3), proteins unique to MG-EVs (Supplementary File S4), and proteins that showed differential quantitative enrichment by 1.5 fold (Supplementary File S5) were used to analyze the enrichment of the protein based on biological function, molecular function, and protein class, using Panther 19.0 (<https://pantherdb.org>; version released 20 June 2024 [27]) based on the available *I. scapularis* genome. Statistical significance was evaluated using Fisher exact test and corrected using a false discovery rate (FDR) of less than 0.05. Fold enrichment values were graphed with GraphPad version 10.4.1 (Prism).

## 2.3. Western Blot Analysis

Western blot analysis was used to confirm the presence of Hsp70, a protein enriched in small and large exosomes [28], and the absence or minimal presence of Calnexin, part of the endoplasmic reticulum but only present in some EV populations [29]. Proteins from EVs and organs were processed and separated by sodium dodecyl sulfate (SDS)-polyacrylamide gel electrophoresis (PAGE) as we previously described [22]. Proteins were transferred onto Immun-Blot® polyvinylidene fluoride (PVDF) membrane sandwiches (Bio-Rad, Hercules, CA, USA, 1620219) and blocked overnight with 5% dry milk (Research Products International; Mount Prospect, IL, USA, M17200-500) in 1X PBS. Membranes were probed with rabbit anti-Hsp70 polyclonal antibodies (1:20,000; ProteinTech, Rosemont, IL, USA; #10995-1-AP) or rabbit anti-Calnexin polyclonal antibodies (1:10,000; Millipore sigma; Saint Louis, MO, USA; AB2301) diluted in 10 mL 1X PBS + 25 µL 5% milk + 5 µL Tween 20 and detected with goat anti-rabbit polyclonal antibodies horse-radish peroxidase (HRP) labeled (1:10,000; Abcam; Waltham, MA, USA; AB6721) diluted in 10 mL 1X PBS + 25 µL 5% milk + 5 µL Tween 20. Bands were detected with Pierce® ECL Western Blot Substrate (Thermo Fisher Scientific) and visualized in an Azure 300 Imager (Azure Biosystems, Dublin, CA, USA). The density of the bands was measured with ImageJ version 1.54g using the gel plot function.

## 2.4. Immunoprecipitation and Label-Free Quantification of Antigenic Proteins

Serum samples from pre-vaccination and 7 days post-3rd booster (day 57 of the study) were obtained from three WTD vaccinated with SG- and MG-EVs (#924, #929, and #934) and one control WTD (#930) from our previous study [22]. These sera were submitted to the Gehrke Proteomics Center at the University of Missouri along with SG- and MG-EVs for immunoprecipitation and proteomic analysis of proteins bound by antibodies (antigenic). Identification of antigenic proteins with animal serum #929 and control (WTD #930) was performed on a different occasion from the immunoprecipitation with serum samples #924, #934, and control #930. The procedures for both immunoprecipitation experiments are described below.

### 2.4.1. Immunoprecipitation

*Immunoprecipitation #929/930:* MG-EVs (60  $\mu$ L) and SG-EVs (75  $\mu$ L) were combined 1:1 with proteinA equilibration buffer before freeze/thawing three times, followed by sonication in a water bath for 5 min three times. Samples were aliquoted in triplicate (18  $\mu$ L for MG-EVs and 20  $\mu$ L for SG-EVs) and incubated with pre-vaccination serum (4  $\mu$ L for WTD#929 serum or 8  $\mu$ L for WTD#930 serum) at 4  $^{\circ}$ C for 1 h at mild agitation. Pierce<sup>TM</sup> Protein A/G Agarose (Thermo Fisher Scientific; Waltham, MA, USA; #20421) was pre-equilibrated by washing three times in buffer. Fifty (50)  $\mu$ L of 50% Protein A/G Agarose was added into each sample and incubated for 30 min at 4  $^{\circ}$ C. Samples were centrifuged for 5 min at 2000 $\times$  g and flow through was recovered. Protein A/G agarose-EV-pre-vaccination complexes were retained to identify potentially sticky proteins and unspecific identifications. The flow-through was incubated with post-vaccination serum (10  $\mu$ L for WTD#929 serum or 9  $\mu$ L for WTD#930 serum) at 4  $^{\circ}$ C for 1 h at mild agitation. Protein A/G Agarose was added (50  $\mu$ L of 50%) and incubated for 30 min at 4  $^{\circ}$ C. Samples were centrifuged for 10 min at 16,000 $\times$  g. Precipitates were washed 3 times with equilibration buffer followed by 3 x washes with 1x PBS.

*Immunoprecipitation #924/934/930:* Immunoprecipitation was performed as detailed above, except that 95  $\mu$ L of MG-EVs and SG-EVs were combined with proteinA equilibration buffer 1:1 and 30  $\mu$ L were equally aliquoted in duplicates. An equal volume of pre-vaccination serum (10  $\mu$ L) and post-vaccination serum (10  $\mu$ L) was used for each animal (WTD #924, #934, and control WTD#930).

### 2.4.2. Mass Spectrometry

Immunoprecipitates were digested on beads with trypsin and peptides were desalted using C18 tips (Pierce). The eluates were lyophilized and resuspended in 10  $\mu$ L of 5% acetonitrile and 0.1% formic acid.

*LC/MS:* Samples immunoprecipitated with serum from vaccinated WTD #929 and #930 were originally acquired using data-dependent acquisition (DDA). LC/MS acquisition was performed as follows: PASEF and TIMS were set to “on”. One MS and ten PASEF frames were acquired per cycle of 1.17 s (~1 MS and 120 MS/MS). Target MS intensity for MS was set at 10,000 counts/s with a minimum threshold of 250 counts/s. A charge-state-based rolling collision energy table was used from 76–123% of 42.0 eV. An active exclusion/reconsider precursor method with release after 0.4 min was used. If the precursor (within mass width error of 0.015  $m/z$ ) was >4X signal intensity in subsequent scans, a second MSMS spectrum was collected. Isolation width was set to 2 (<700  $m/z$ ) or 3 (800–1500  $m/z$ ). This allowed us to identify precursors to reduce error during data-independent acquisition (DIA).

Samples immunoprecipitated with serum from vaccinated WTD #929 were later analyzed using DIA settings, as follow: 1  $\mu$ L of resuspension was loaded onto a pepsep25 col-



umn (25 cm × 75 µm × 1.9 µm ReproSil-AQC18; Bruker). Peptides were separated with a gradient of acetonitrile at 300 nL/min with the following LC gradient conditions: initial conditions were 3% B (A: 0.1% formic acid in water, B: 99.9% acetonitrile, 0.1% formic acid), followed by 10 min gradient to 17% B. Then 17–25% B over 5 min, 25–37% B over 5 min, 37–80% B over 3 min, end with three flushing cycles (80–40% B for 1 min), and finally back to initial conditions (3% B) for 1 min and hold for 2 min to equilibrate the column. The total run time was 30 min. MS data were collected using DIA-PASEF over an  $m/z$  range of 300.5 to 1349.5 and a mobility range of 0.65 to 1.45. Fifty DIA windows were collected (of varying  $m/z$  width) for a total cycle time of 2.76 s. An ion-mobility-based collision energy was used with 20 eV at 0.85 and 59 eV at 1.30. This procedure using DIA settings was also used for samples immunoprecipitated with WTD #924, #934, and #930 but was completed on a different date.

#### 2.4.3. Data Analysis

Data acquired during DDA LC/MS were submitted to the PEAKS-11 search engine for protein identifications. The NCBI-Ixodes database was searched with trypsin-specific as enzyme, allowing for 2 missed cleavages, and using carbamidomethyl-Cys as fixed modification and oxidized methionine as variable modification. The mass tolerance for precursor ions was set at 20 ppm and 0.1 Da on-fragment ions. A decoy database was automatically generated and searched for FDR calculation. Search results files were filtered for 0.1% FDR (peptide false discovery rate).

The raw data were copied to Spectronaut V18 (Biognosis Inc., Zurich, Switzerland) server and searched against an NCBI-Ixodes FASTA database using the direct DIA approach incorporating the Pulsar algorithm. Spectronaut default parameters were used for the search with trypsin as enzyme, Carbamidomethyl-Cys as fixed modification, and Oxidized-Met and deamidated-NQ as variable modifications. Protein quantity was reported as MS2Quantity (sum of peptide fragments intensities from collision-induced dissociation (CID) MS/MS matching each protein). Quantitative data from WTD #924/934/930 immunoprecipitations were statistically evaluated as follows: data (MS2Quantity, sum of peptide fragment abundances per protein) were imported into Perseus V16.0.1 and grouped into 12 groups (3 “pre” SG and MG; and 3 “vacc” MG and SG). Data were filtered for an MS2Quantity of  $\geq 10$  in two samples of at least one group and data sum normalized (protein abundance/total abundance) in each sample. *T*-tests were then conducted with two valid values in at least one group to compare pre- and post-vaccine for each animal and each tissue sample. The DIA-PASEF mass acquisition for the immuno-precipitates with WTD #929 serum resulted in high variation and could not be analyzed statistically.

#### 2.5. Data Availability

The mass spectrometry proteomics data associated with this manuscript have been deposited to the ProteomeXchange Consortium via PRIDE [30] repository with the dataset identifier PXD058874.

#### 2.6. Antigens Classification

Proteins identified during the immunoprecipitation were classified into three different groups: high, medium, and low priority, using the criteria described below.

High priority: Proteins were precipitated with at least two vaccinated WTD serum samples; proteins were identified in the samples precipitated with post-vaccinated serum and not present in pre-vaccination pool (unique to vaccinated); statistically significant by adjusted *t*-test analysis; and absent in precipitates using control serum (WTD #930).

Medium priority: Proteins were precipitated with at least two vaccinated WTD serum samples; proteins were  $\geq 5$ -fold enriched in precipitates processed with post-vaccination

serum when compared to pre-vaccination serum; statistically significant by adjusted *t*-test analysis; and absent in precipitates using control serum (WTD #930).

Low priority: Proteins were precipitated with at least two vaccinated WTD serum samples; proteins were identified in the samples precipitated with post-vaccinated serum and not present in pre-vaccination pool (unique to vaccinated); however, proteins presented variability in spectra intensity levels and were not significant by adjusted *t*-test analysis; and absent in precipitates using control serum (WTD #930).

The potential identity of proteins without known function (hypothetical or putative proteins) was investigated by Position specific iterated (PSI) Basic Local Alignment Search Tool (BLAST) [URL <https://blast.ncbi.nlm.nih.gov/>; accessed on 15 November 2024] using *I. scapularis* as the target species.

### 3. Results

#### 3.1. Extracellular Vesicles Secreted by Different Organs Share a Core Set of Proteins

Recent studies demonstrate that certain proteins are associated with vesicle subtypes independent of the secreting cell origin [28]. These proteins can be used as markers to classify the different EV subpopulations and the International Society for Extracellular Vesicles (ISVE) has designated them for the validation of EVs' identities [29]. Although our and other studies identified several of these markers in salivary and hemolymph EVs, using Western blotting and proteomic analysis [23–25], it remained to be determined whether tick vesicles secreted by different organs shared a core proteomic cargo. Proteomic analysis of the SG- and MG-EVs used for our previous vaccination experiments [22] identified 1539 proteins (Supplementary File S1). From these, 914 and 360 proteins were present in all biological and technical replicates of MG- and SG-EVs, respectively (Figure 1A). To determine the core protein cargo transported within *A. americanum* SG- and MG-EVs, we compared the proteins identified in all technical and biological replicates in each EV type. This core cargo consisted of 340 proteins that were shared between SG- and MG-EVs (Figure 1A; Supplementary File S2). Enrichment analysis of the proteins found within the core cargo shows an over-representation of proteins involved in glycogen metabolic process (GO:0005977), barbed-end actin filament capping (GO:0051016), purine metabolic process (GO:0009167), and other metabolic processes (Figure S1A). Molecular functions that were enriched included constituents of ribosome (GO:0003735), translation elongation factor (GO:000374), ATP binding (GO:0005524), proteins disulfide isomerase activity (GO:0003756), and included GTPase activity (GO:0003924) (Figure S1B). Among the protein class enriched within both vesicles chaperonin (PC00073), Hsp90 family chaperone (PC00028), Hsp70 family chaperone (PC00027), actin and actin-related protein (PC00039), ribosomal proteins (PC00202), vesicle coat proteins (PC00235), small GTPases (PC00208), and others were identified (Figure 1B). The presence of Hsp70 within both EVs samples was confirmed by Western blot analysis, as well as the absence of the endoplasmic reticulum protein Calnexin (Figure 1C). This confirms that several markers used to classify EVs in other systems are shared among vesicles secreted by different organs in *A. americanum*.

#### 3.2. Unique and Differentially Expressed Proteins Within Midgut Extracellular Vesicles Mirror Organ Functions

Although we identified a core set of proteins that were shared between vesicles from different organs, several of the proteins packed within them were unique to each vesicle type [20 proteins in SG-EVs (Supplementary File S3) and 574 in MG-EVs (Supplementary File S4; Figure 1A)]. Nevertheless, the unique proteins in MG-EVs appear to reflect the function of the tissue secreting them. Enrichment analysis shows that the biological processes with the highest fold enrichment in MG-EVs were exocytic process (GO:0140029), vacuolar

acidification (GO: 0007035), mitochondrial fusion (GO:0008053), IMP metabolic process (GO:0046040), and clathrin-dependent endocytosis (GO:0072583; Figure 2). Among the enriched molecular functions (Figure S2A), non-membrane spanning protein kinase activity (GO: 0004715), syntaxin binding (GO: 0019905), and sterol transporter activity (GO:0015248) were the most enriched; however, proteins with hydro-lyase activity (GO:0016836) and oxidoreductase activity (GO:0016616) were also enriched. This enrichment suggests a potential role of tick EVs in digestion and detoxification of the blood meal. The enriched protein classes found within MG-EVs are presented in Figure S2B and include heterotrimeric G-protein (PC00117), membrane trafficking regulatory protein (PC00151), dehydrogenase (PC00092), and lyase (PC00144).

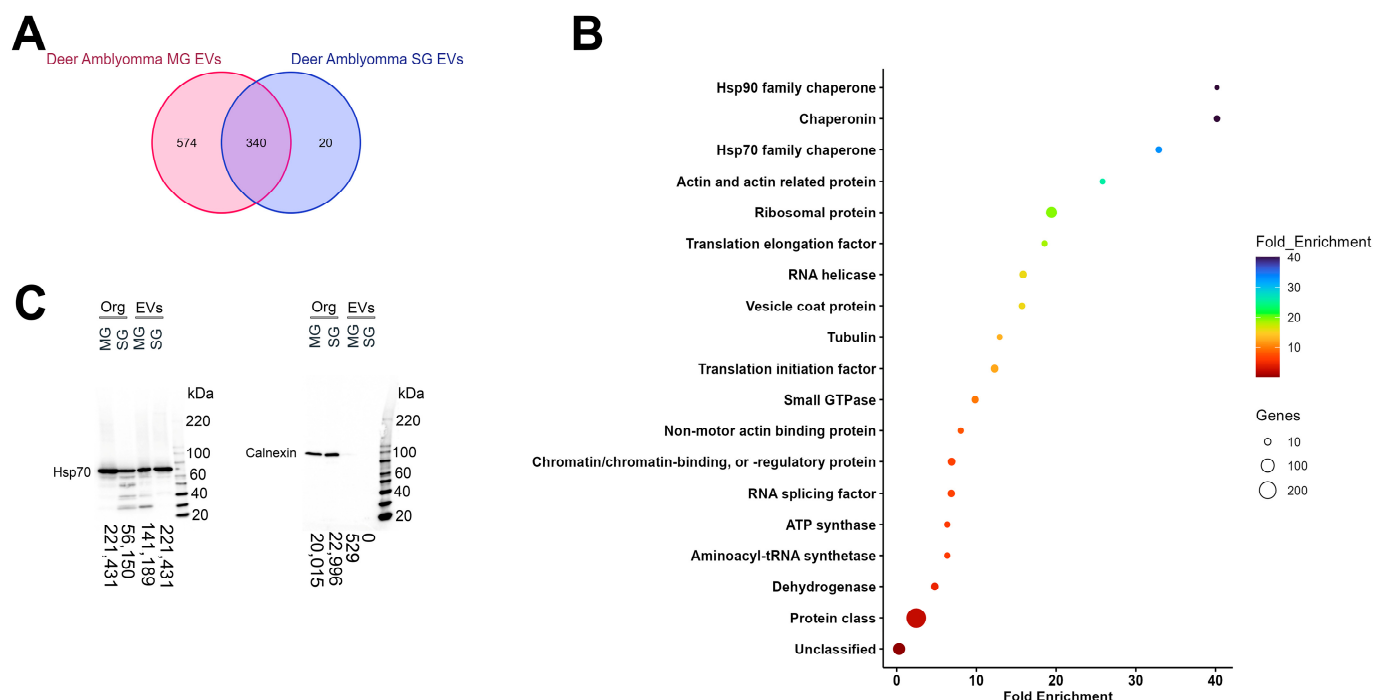


**Figure 1.** Shared proteomic cargo packed within salivary and midgut extracellular vesicles secreted by *Amblyomma americanum* females fed on white-tailed deer. Extracellular vesicles (EVs) from salivary glands (SG) and midguts (MG) were characterized by mass spectrometry using parallel accumulation–serial fragmentation (PASEF) in a Bruker timsTOF-PRO. **(A)** Venn diagrams representation of unique and shared proteins found within SG-EVs (blue) and MG-EVs (red). **(B)** Enrichment analysis of protein classes shared between *A. americanum* SG- and MG-EVs. Bars represent the fold enrichment with  $p$ -value  $\leq 0.05$  and false discovery rate (FDR)  $\leq 0.05$ . **(C)** Western blot analysis of heat shock protein 70 (Hsp70) and Calnexin in midgut (MG) and salivary gland (SG) organs (Org) and extracellular vesicles (EVs). Proteins (50  $\mu$ g for organs and 15  $\mu$ g for EVs) were separated by SDS-PAGE and transferred into membranes. Numbers next to the ladder represent the size in kilodaltons (kDa). Hsp70 estimated size = ~70 kDa. Calnexin estimated size = ~90 kDa.

Of the 1539 proteins detected in both vesicle types, only 516 were quantifiable and 333 were differentially abundant by Student's  $t$ -test  $q$ -value (Benjamini–Hochberg correction = 0.05). This included 165 more abundant proteins in MG-EVs and 166 proteins were more abundant in SG-EVs (Figure 3A and Supplemental File S5). Enrichment analysis of the proteins differentially expressed in both vesicle populations show potentially different roles for each vesicle type. MG-EVs were enriched in proteins involved in glutamate metabolic process (GO:0006536), clathrin-dependent endocytosis (GO:0072583), protein N-linked glycosylation (GO:0006487), and other processes (Figure 3B). These processes differed from those proteins over-represented in SG-EVs, which included nucleosome assembly (GO: 0006334), regulation of canonical Wnt signaling pathway (GO:0060828), purine ribonucleo-



side monophosphate metabolic process (GO:0009167), and others (Figure 3C). Interestingly, except for translation elongation (GO:0006414) and protein folding (GO:0006457), all biological processes enriched within the differentially abundant proteins differed between EV populations, likely due to their distinct function. Likewise, little overlap was observed in Gene Ontology (GO) on the molecular function of proteins differentially abundant in MG-EVs versus SG-EVs, with only actin filament binding (GO:0051015) and translation initiation factor activity (GO:0003743) being shared (Figure S3A,B). Nevertheless, several proteins classes were enriched within the overabundant proteins in both vesicle populations, including translation initiation factors (PC00222), vesicle coat protein (PC00235), RNA splicing factor (PC00148), and RNA helicase (PC00148) (Figure S3C,D).

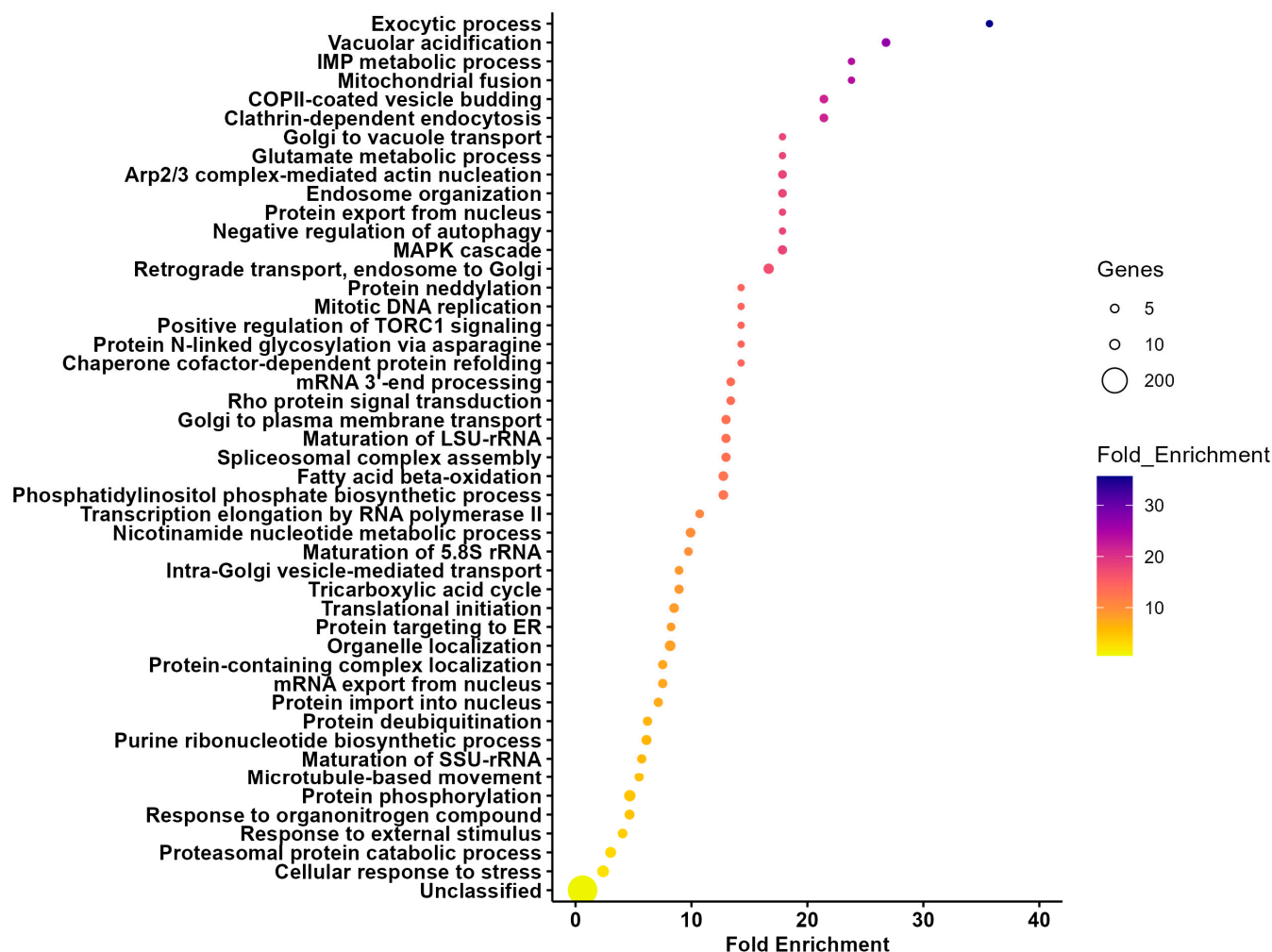


**Figure 2.** Enrichment analysis of proteins unique to extracellular vesicles (EVs) secreted by midguts from *Amblyomma americanum*. Proteins identified in EVs secreted by ex vivo midgut organ cultures from *A. americanum* females fed on white-tailed deer were compared to those from salivary gland EVs to identify unique proteins. An enrichment analysis of biological functions was performed in these unique proteins using Panther. Bars represent the fold enrichment with  $p$ -value  $\leq 0.05$  and false discovery rate (FDR)  $\leq 0.05$ .

### 3.3. Salivary Gland-Derived Extracellular Vesicles Contain More Antigenic Proteins than Midgut Vesicles

In our previous study, we visualized several antigenic proteins within MG- and SG-EVs using Western blot analysis. This included several bands that appeared consistently in all blots probed with serum from vaccinated animals and serum from animals after tick infestation [22]. To identify these proteins, immuno-precipitations were performed at the

Gehrke Proteomics Center at the University of Missouri using pre- and post-vaccination sera from vaccinated WTD #929 and one control WTD (#930), originally. Pre-vaccinated serum was used to identify sticky proteins and proteins naturally recognized by the host. The pre-cleared lysates were then used to precipitate antigenic proteins using the serum of the vaccinated animal (#929) from 7 days after the last booster [22]. The same approach was performed using serum from a control animal injected with adjuvant only (WTD #930). These proteins were identified by data-dependent acquisition (DDA) (Supplementary File S6). No proteins were consistently precipitated with the post-injection sera from the control animal (WTD# 930). A total of ten proteins were uniquely found with the post-vaccination serum of WTD #929, including six from SG-EVs and four from MG-EVs. The proteins precipitated from SG-EVs lysates consisted of two alpha-macroglobulins (JAT97670.1 and JAT93800.1), a hypothetical protein (AOE35522.1) that is homolog to a nucleoside diphosphate kinase from *I. scapularis* (XP\_002416191.1), a conserved secreted protein (JAT93667.1) without homology to proteins with known function, vitellogenin-1 homolog (AXP34687.1), and an alpha-glucosidase-like enzyme (XP\_029834972.1). Antigenic proteins identified from MG-EVs included vitellogenin-2 (JAU01362.1), an acid phosphatase (JAT99430.1), a conserved secreted protein (JAU00577.1), and a hypothetical protein (JAP80714.1) of unknown function (Table 1).

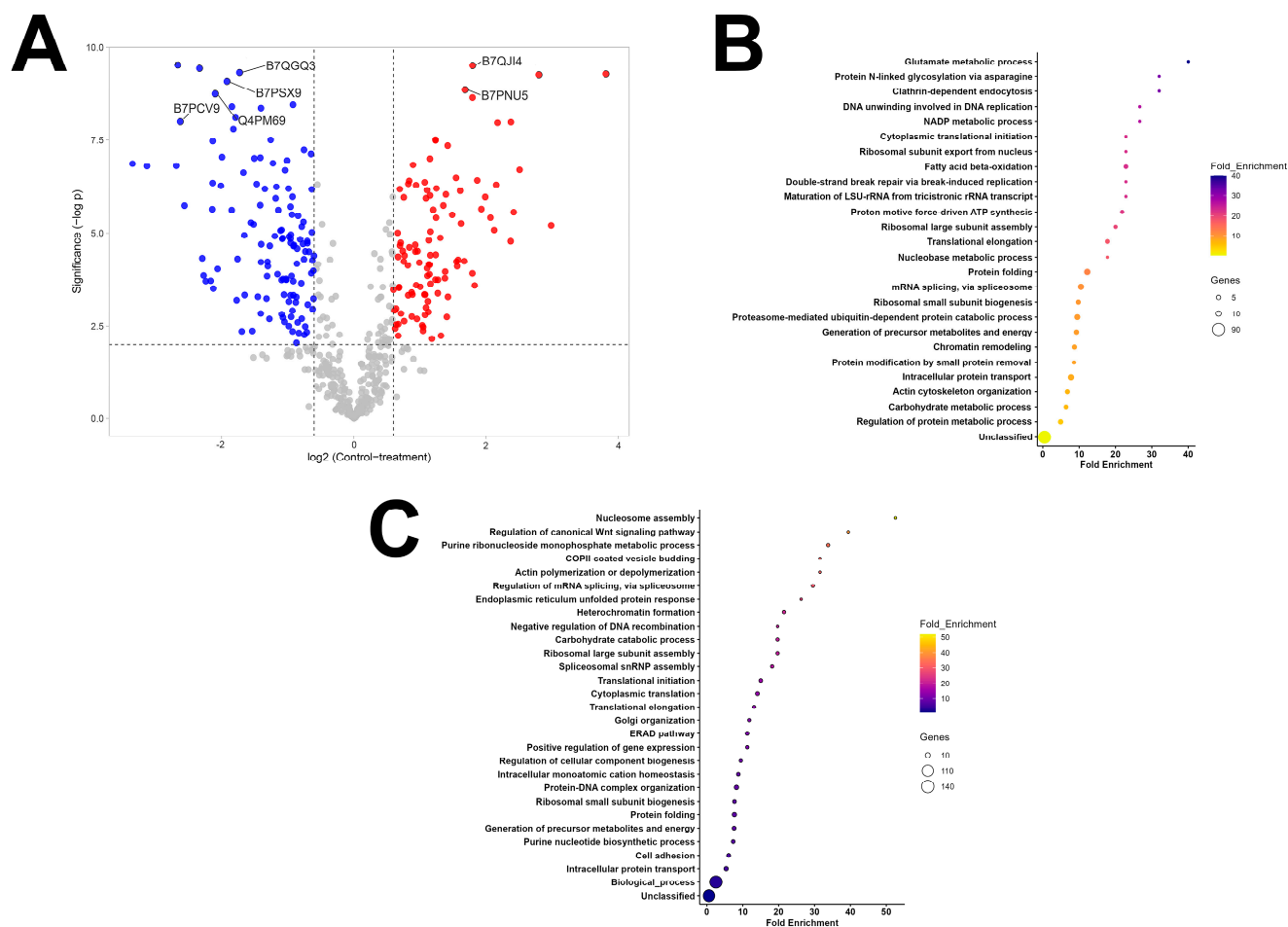


**Figure 3.** Differentially abundant proteins in extracellular vesicles secreted by midgut and salivary glands from *Amblyomma americanum*. (A) Volcano plot of differentially abundant proteins with 1.5—fold cut off. Proteins in blue represent overabundant proteins in salivary glands extracellular vesicles (SG-EVs), whereas proteins in red are more abundant in midgut extracellular vesicles (MG-EVs). Enrichment analysis of the biological function of proteins overabundant in (B) MG-EVs or (C) SG-EVs. Bars represent the fold enrichment with  $p$ -value  $\leq 0.05$  and false discovery rate (FDR)  $\leq 0.05$ .

**Table 1.** Antigenic proteins identified in salivary and midgut extracellular vesicles from *Amblyomma americanum* females by data-dependent acquisition (DDA) using serum from white-tailed deer #929.

Protein Accession	Protein Name (Tick Species)	Vesicle Type
JAT97670.1	Putative alpha-macroglobulin, partial ( <i>Amblyomma aureolatum</i> )	Salivary
JAT93800.1	Putative alpha-macroglobulin, partial ( <i>Amblyomma aureolatum</i> )	Salivary
AEO35522.1	Hypothetical protein ( <i>Amblyomma maculatum</i> )	Salivary
JAT93667.1	Putative conserved secreted protein precursor ( <i>Amblyomma aureolatum</i> )	Salivary
AXP34687.1	Vitellogenin-1 ( <i>Haemaphysalis flava</i> )	Salivary
XP_029834972.1	Lysosomal alpha-glucosidase-like, partial ( <i>Ixodes scapularis</i> )	Salivary
JAU01362.1	Putative vitellogenin-2, partial ( <i>Amblyomma sculptum</i> )	Midgut
JAT99430.1	Putative lysosomal acid phosphatase, partial ( <i>Amblyomma sculptum</i> )	Midgut
JAU00577.1	Putative conserved secreted protein precursor, partial ( <i>Amblyomma sculptum</i> )	Midgut
JAP80714.1	Hypothetical protein ( <i>Rhipicephalus appendiculatus</i> )	Midgut

Due to the drawbacks of the DDA approach, including lower sensitivity, accuracy, and reproducibility [31], the WTD #929 immuno-precipitations were re-acquired using data-independent acquisition (DIA). The identification of antigens precipitated with the serum from vaccinated WTD #924 and #934 and control #930 were also completed using this approach (Supplementary Files S7 and S8). DIA allows for unbiased identification of proteins by separating precursors in small windows and identifying all product ions from those windows [31]. Using this approach, we categorized antigens into three groups: “high-priority”, “medium-priority”, and “low-priority” antigens. Proteins were considered high-priority antigens (Table 2) when they were precipitated with post-vaccination serum from treated animals only and had little variation in the spectral intensities, presenting statistical significance. Due to the high variations in the MS-DIA performed with WTD #929, only proteins recognized by WTD#924 and WTD #934 were evaluated in this group (Supplemental File S7). Curiously, only one midgut EV protein was identified, a hypothetical protein (JAT95206.1) with homology to a mucin protein (mucin-2) in *I. scapularis* (XP\_029828425.2). In comparison, seven high priority proteins were associated with salivary EVs precipitates, including three enzymes (JAG92630.1, JAT95172.1, and JAU00888.1), two hypothetical proteins (JAT95331.1 and JAP80714.1), none of which have homology with proteins of known function in *I. scapularis*, a conserved secreted protein (JAU00577.1) with no homology to proteins with known function in *I. scapularis*, and protein in meprin (JAU00890.1) (Table 2), homolog to an apical endosomal protein that may function as a low-density lipoprotein receptor in *I. scapularis* (XP\_040066431.1). These proteins represent strong candidates for future testing.

Proteins that were uniquely precipitated with the vaccinated serum of treated animals, but that show high levels of variation in spectral levels and, therefore, did not achieve statistical significance were grouped into medium-priority antigens (Table 3). This included proteins identified by DIA in WTD #929 (Supplemental File S8). As in the previous group, most of the proteins were precipitated from SG-EV lysates (five proteins). Two midgut proteins were identified, including JAT94005.1, which is a putative secreted mucin that has homology to an elastin-like protein in *I. scapularis* (XP\_040078974.1), and JAU02543.1, a hypothetical protein with no homology to proteins in *I. scapularis*. Among the SG-EV proteins precipitated, we discovered three enzymes (JAT97490.1, JAP66750.1, and JAP71591.1), a

Hemicentin (XP\_029824064.1), and a plasma membrane protein (JAU01951.1), which is a homolog to prominin-1-A [a transmembrane glycoprotein] in *I. scapularis* (XP\_042142011.1). The last group of antigens consisted of proteins that were  $\geq 5$  fold enriched in the precipitates from vaccinated animals and presented statistical significance in their spectral increases (Table 4). Although it was the largest group of proteins (16 total), these were considered low priority antigens as peptides from these proteins were detected in some precipitates from the pre-vaccinated serum. These proteins were all identified in the SG-EV precipitates and included eight enzymes (JAP82974.1, JAT95210.1, AEO36445.1, JAT95556.1, JAU00184.1, JAP80906.1, JAT97770.1, and JAT97963.1), two hypothetical proteins (JAU00361.1 and JAP83809.1), two vitellogenins (JAU01916.1 and AJR36491.1), an alpha-macroglobulin (JAT93800.1), a putative tetraspanin (JAG92577.1), a putative secreted protein (JAT92299.1) with unknown function, and a putative protein (AEO35082.1), which is homologous to N(4)-(Beta-N-acetylglucosaminy)-L-asparaginase in *I. scapularis* (XP\_029825395.3).

**Table 2.** High-priority antigens identified in extracellular vesicles secreted by midguts and salivary glands from *Amblyomma americanum* females fed on white-tailed deer.

Protein Accession #	Protein Name (Tick Species)	Vesicle Type
JAT95206.1	Hypothetical protein, partial ( <i>Amblyomma aureolatum</i> )	Midgut
JAG92630.1	Putative peptidase family m2 angiotensin converting enzyme, partial ( <i>Amblyomma aureolatum</i> )	Salivary
JAT95172.1	Putative catalytically inactive chitinase-like lectin, partial ( <i>Amblyomma aureolatum</i> )	Salivary
JAT95331.1	Hypothetical protein, partial ( <i>Amblyomma aureolatum</i> )	Salivary
JAU00577.1	Putative conserved secreted protein precursor, partial ( <i>Amblyomma sculptum</i> )	Salivary
JAU00888.1	Putative alpha-d-galactosidase melibiase, partial ( <i>Amblyomma sculptum</i> )	Salivary
JAU00890.1	Protein in meprin, partial ( <i>Amblyomma sculptum</i> )	Salivary
JAP80714.1	Hypothetical protein ( <i>Rhipicephalus appendiculatus</i> )	Salivary

**Table 3.** Medium-priority antigens identified in extracellular vesicles secreted by midguts and salivary glands from *Amblyomma americanum* females fed on white-tailed deer.

Protein Accession #	Protein Name (Tick Species)	Vesicle Type
JAT94005.1	Putative secreted mucin muc17, partial ( <i>Amblyomma aureolatum</i> )	Midgut
JAU02543.1	Hypothetical protein, partial ( <i>Amblyomma sculptum</i> )	Midgut
JAT97490.1	N-acylsphingosine amidohydrolase acid ceramidase, partial ( <i>Amblyomma aureolatum</i> )	Salivary
XP_029824064.1	Hemicentin-2 putative, partial ( <i>Ixodes scapularis</i> )	Salivary
JAP66750.1	Metalloprotease atp-dependent zinc metalloprotease yme1 protein isoform x1, partial ( <i>Hyalomma excavatum</i> )	Salivary
JAP71591.1	LOW glucosidase ii catalytic alpha subunit, partial ( <i>Ixodes ricinus</i> )	Salivary
JAU01951.1	Putative conserved plasma membrane protein, partial ( <i>Amblyomma sculptum</i> )	Salivary

**Table 4.** Low-priority antigens identified in extracellular vesicles secreted by salivary glands from *Amblyomma americanum* females fed on white-tailed deer.

Protein Accession #	Protein Name (Tick Species)	Vesicle Type
JAT93800.1	Putative alpha-macroglobulin, partial ( <i>Amblyomma aureolatum</i> )	Salivary
JAP82974.1	Uncharacterized alpha-mannosidase ( <i>Rhipicephalus appendiculatus</i> )	Salivary
JAT95210.1	Putative glucosidase ii catalytic alpha subunit, partial ( <i>Amblyomma aureolatum</i> )	Salivary
JAU00361.1	Hypothetical protein, partial ( <i>Amblyomma sculptum</i> )	Salivary
AEO36445.1	Endochitinase-like protein ( <i>Amblyomma maculatum</i> )	Salivary
JAP83809.1	Hypothetical protein ( <i>Rhipicephalus appendiculatus</i> )	Salivary
JAT95556.1	Putative aminopeptidase ( <i>Amblyomma aureolatum</i> )	Salivary
JAU00184.1	Putative catalytic domain of lysosomal alpha-mannosidase, partial ( <i>Amblyomma sculptum</i> )	Salivary
JAP80906.1	Lysosomal acid phosphatase ( <i>Rhipicephalus appendiculatus</i> )	Salivary
JAG92577.1	Putative tetraspanin ( <i>Amblyomma americanum</i> )	Salivary
JAU01916.1	Putative vitellogenin-b ( <i>Amblyomma sculptum</i> )	Salivary
JAT97770.1	Putative leucine aminopeptidase, partial ( <i>Amblyomma aureolatum</i> )	Salivary
JAT97963.1	Putative alpha-amylase, partial ( <i>Amblyomma aureolatum</i> )	Salivary
AJR36491.1	Vitellogenin-6 CP3 ( <i>Ixodes ricinus</i> )	Salivary
JAT92299.1	Putative secreted protein, partial ( <i>Amblyomma aureolatum</i> )	Salivary
AEO35082.1	Putative protein ( <i>Amblyomma maculatum</i> )	Salivary

#### 4. Discussion

Different strategies have been developed for the discovery of anti-tick antigens, including reverse vaccinology based on proteomic and genomic data [32], purification of single proteins from organ and tissue extracts [33], in silico immunogenicity analysis of individual proteins [34], or by the selection of individual proteins based on experimental validation of their function [35]. However, some of the drawbacks of these approaches are the time it takes to validate single targets, the lack of the functional characterization of the immune system of WTD for the use of reverse vaccinology and in silico testing in this system, and little information on protein expression during tick feeding on wildlife hosts. Unlike in model organisms, only a few studies have characterized genetic and cellular traits associated with immune resistance against parasites and microbes in WTD [36–38]. Further, the genetic structure of the major histocompatibility complex II (MHC II) in ruminants differs from other mammals and WTD have high MHC II polymorphism in *DRB* [39], likely to affect how populations respond to antigens within a vaccine. Given that most vaccine design tools available have been tailored towards humans, animal models, or live-stock [40–42], different approaches may be necessary to discover antigens that are reliable for the development of anti-tick vaccines targeting WTD. The goal of the present study was to leverage serum generated in our previous study [22] to identify proteins in tick SG- and MG-EVs recognized by the immune system of vaccinated WTD using immunoprecipitation and LC-MS/MS to pinpoint proteins that can be further evaluated as vaccine candidates against ticks in this important reproductive host.

This strategy has previously been employed to pinpoint antigens recognized by the immune response of cattle after vaccination with *I. ricinus* midgut and salivary extracts [43]. Given that the proteins in the high-priority list represent those that are unique to the



vaccinated serum and show little variability, these proteins are the vaccine candidates with the most potential and that should be further tested. Among these proteins, a putative alpha-d-galactosidase melibiase (JAU00888.1) is of particular interest as it may naturally lead to hypersensitivity to red meat that has been associated with *A. americanum* bites in humans. A recent study showed that alpha-d-galactosidase might be involved in the production of N-glycans and other sugar modifications in proteins and other molecules that are injected into the host with tick saliva [44]. Sugar modifications, such as alpha gal, fucosylation, and sialic acids are important for the transmission of tick-borne pathogens and to stimulate the immune response against ticks [45,46]. Interestingly, silencing of this enzyme in ticks has a favorable effect on tick-feeding, possibly by reducing basophil activation [44]. Basophils are known to be important for anti-tick immunity potentially by interacting with IgE and degranulating [47], which can lead to further cellular infiltration and itchiness. In fact, during experimental infestations in our previous study, we lost many ticks due to grooming [22], likely a pruritic effect of tick feeding.

Another enzyme that needs further testing is putative catalytically inactive chitinase-like lectin, partial (JAT95172.1). Chitinases have a wide array of functions in insects, from assistance in molting to immune responses [48]. A tick chitinase has previously been tested as a vaccine candidate against *Haemaphysalis longicornis* infestations in mice, leading to protective immunity and delays in molting and egg weight [49]. Whether the present chitinase is involved in molting remains to be determined since it is presumably catalytically inactive. Catalytically inactive chitinases have previously been shown to play a role as growth factors or in immunity [48]. There is a possibility that this chitinase completes a different function. In fact, vaccination of deer with SG- and MG-EVs deer did not have any effect on nymph molting to adult [22]. Thus, further characterization of this protein's function is warranted to fully determine its potential as vaccine candidate. Nevertheless, most of the proteins discovered, independently of the priority group that the proteins belonged to, in this study consisted of hypothetical proteins (10 total), putative secreted proteins, and other proteins without known function, highlighting our still poor understanding of tick biology. The functional characterization of the proteins identified herein will serve twofold: (1) it will allow us to further determine their potential as vaccine candidates, and (2) increase our knowledge on tick biology. Likewise, except for JAU00888.1, which was recently characterized and shown to affect tick feeding [44], the other proteins within our high-priority list should be functionally characterized to understand their biological significance.

Extracellular vesicles are important for tick feeding [24] and previous experiments show that ovaries can uptake EVs circulating in tick hemolymph [25]. Interestingly, our proteomic analysis of MG-EVs demonstrates that several of the proteins that are unique to this vesicle type are involved in metabolism, vacuolar acidification, and endocytosis. Ticks complete the digestion of the blood meal intracellularly after digestive cells endocytose the blood meal and form organelles called hemosomes. The blood meal breakdown is performed by acidic peptidases [50]. We suspect that unique cargo within MG-EV indicates their potential role in tick digestion. Future experiments should evaluate the expression and function of these proteins, as well as evaluate their efficacy as part of a multivalent vaccine. Extracellular vesicles have a role in activating and modulating immune responses by trafficking and exchanging multiple antigens between cells [51]. The antigens described herein might overcome the disadvantages experienced with previous multivalent vaccine tests, such as antigenic competition [52]. These proteins can be transfected within suspension cells, such as FreeStyle™ 293-F cells, to produce engineered extracellular vesicles [53], or they could be deposited within hybrid mimic extracellular vesicles constructed based on mix of liposomes and tick EV membranes [54]; also, the mRNA encoding these proteins

could be transfected into plant-derived EVs [55]. These approaches will allow for the improvement in mass production and even the potential oral delivery of the vaccine [54,55], which would facilitate the vaccination of large number of animals by using oral delivery. Vaccinations through the oral route have been used for the control of *B. burgdorferi* in the wild-rodent reservoir and tick populations [56] and for the application of Rabies vaccine to wildlife, a USDA program that has been highly successful [57], thus, demonstrating the feasibility of an oral administration for the vaccine, even though it is unknown whether this route works large wild reservoirs or when excess of other food options are available in the environment.

One limitation of the present study is the small sample set (three vaccinated and one control WTD), which is due to the complexities of working with ungulate hosts, including the cost to purchase, raise, and maintain WTD in tick-free conditions to ensure that pre-vaccination serum does not deplete the samples from naturally immunogenic proteins. These results provide proof-of concept that studies to identify tick antigens can be conducted in these targeted host animals, leading to the discovery that EVs (1) have shown protection against ticks in the target host and (2) are known to be expressed during feeding in the target host. This approach can be used to identify extracellular vesicle proteins that are immunogenic to other species, such as cattle, other reservoir animals, and even humans. Further extracellular proteins that are recognized by multiple species could be packed within extracellular vesicles mimics as multivalent vaccines used to immunize different tick hosts.

**Supplementary Materials:** The following supporting information can be downloaded at: <https://www.mdpi.com/article/10.3390/vaccines13040355/s1>, Figure S1: Enrichment analysis of the biological and molecular functions of core proteins within *Amblyomma americanum* extracellular vesicles; Figure S2: Molecular function (A) and protein class (B) enrichment analysis of proteins unique to midgut extracellular vesicles; Figure S3: Molecular function and protein class enrichment analysis of differentially expressed proteins to midgut (A and C) and salivary (B and D) extracellular vesicles; Supplemental File S1: Normalized spectral intensity from LC/MS MG- SG-EV *Amblyomma americanum*; Supplemental File S2: Salivary and midgut EV shared cargo *Amblyomma americanum* WTD; Supplemental File S3: Proteins unique to *Amblyomma americanum* SG-EVs WTD; Supplemental File S4: Proteins unique to *Amblyomma americanum* MG-EVs WTD; Supplemental File S5: Differentially abundant proteins; Supplemental File S6: Immunoprecipitation experiment\_929-930\_SG and MG\_Proteins identified\_DAA; Supplemental File S7: IP-DIA-924\_934\_930\_MG\_SG\_pre and vacc\_proteins identified; Supplemental File S8: IP-DIA-929\_MG\_SG\_pre and vacc\_proteins identified.

**Author Contributions:** Conceptualization, A.O.C.; methodology, A.O.C.; formal analysis, A.O.C. and S.D.; investigation, A.O.C., J.G., C.H., C.d.S.R.-S., B.L.-G., K.A.P., S.D. and T.L.J.; resources, A.O.C., P.U.O. and T.L.J.; data curation, A.O.C. and J.G.; writing—original draft preparation, A.O.C.; writing—review and editing, B.L.-G., J.G., C.d.S.R.-S., T.L.J. and P.U.O.; visualization, A.O.C.; supervision, A.O.C. and T.L.J.; project administration, A.O.C. and T.L.J.; funding acquisition, A.O.C. and T.L.J. All authors have read and agreed to the published version of the manuscript.

**Funding:** This project was supported by the Diseases of Agriculture Animals (A1221) program from the USDA National Institute for Food and Agriculture (NIFA) award #2022-67015-42166 and University of Wisconsin, Madison start-up funds to AOC and USDA NIFA Hatch Project #700738 and Multistate Hatch Project #7007722 to TLJ. BLG is supported by an ORISE fellowship from the USDA and was a recipient of the Knippling–Bushland–Swahrff fellowship from the Department of Entomology at Texas A&M University. CSR-S was supported by Coordenação de Aperfeiçoamento de Pessoal de Nível Superior—CAPES fellowship during her visit to Texas A&M University. SD was supported by EFAS-REEU, grant no. 2016-67032-25013.

**Institutional Review Board Statement:** Not applicable.

**Informed Consent Statement:** Not applicable.

**Data Availability Statement:** The mass spectrometry proteomics data associated with this manuscript have been deposited to the ProteomeXchange Consortium via PRIDE [30] repository with the dataset identifier PXD058874.

**Acknowledgments:** We thank Brian Mooney at Gehrke Proteomics Center at the University of Missouri for the discussions during the design of the study.

**Conflicts of Interest:** Adela Oliva Chavez and Tammi Johnson have invention disclosures with Texas A&M University and the University of Wisconsin, Madison for the use of tick extracellular vesicle-derived proteins for the development of anti-tick vaccines. These disclosures did not affect the performance of these experiments. This article reports the results of research only and mention of a proprietary product does not constitute an endorsement or recommendation by the USDA for its use. USDA is an equal opportunity provider and employer.

## Abbreviations

The following abbreviations are used in this manuscript:

US	United States
WTD	White-tailed deer
SG	Salivary
MG	Midgut
EVs	Extracellular vesicles
PBS	Phosphate-buffered saline
LC	Liquid chromatography
DDA	Data-dependent acquisition
PASEF	Parallel accumulation–serial fragmentation
MS	Mass spectrometry
TIMS	Trapped ion mobility spectrometry
LFQ	Label-free quantification
MBR	Match between runs
NCBI	National Center for Biotechnology Information
PSM	Peptide–spectrum match
Da	Daltons
PVDF	Polyvinylidene fluoride
SDS	Sodium dodecyl sulfate
PAGE	Polyacrylamide gel electrophoresis
HRP	Horse radish peroxidase
DIA	Data-independent acquisition
CID	Collision-induced dissociation
FDR	False discovery rate
PSI	Position specific iterated
BLAST	Basic Local Alignment Search Tool
ATP	Adenosine triphosphate

## References

1. CDC. Tickborne Disease Surveillance Data Summary. Available online: <https://www.cdc.gov/ticks/data-research/facts-stats/tickborne-disease-surveillance-data-summary.html> (accessed on 22 November 2024).
2. Deshpande, G.; Beetch, J.E.; Heller, J.G.; Naqvi, O.H.; Kuhn, K.G. Assessing the Influence of Climate Change and Environmental Factors on the Top Tick-Borne Diseases in the United States: A Systematic Review. *Microorganisms* **2023**, *12*, 50. [CrossRef] [PubMed]
3. Eisen, L. Tick species infesting humans in the United States. *Ticks Tick-Borne Dis.* **2022**, *13*, 102025. [CrossRef] [PubMed]
4. Teel, P.D.; Fuchs, T.W.; Huston, J.E.; Longnecker, M.T.; Pickel, S.L. Effects of sequential infestations of *Dermacentor albipictus* and *Amblyomma americanum* (Acari: Ixodidae) on overwintering beef cows in west-central Texas. *J. Med. Entomol.* **1990**, *27*, 632–641. [CrossRef]

5. Higueta, N.I.A.; Franco-Paredes, C.; Henao-Martínez, A.F. The expanding spectrum of disease caused by the Lone Star Tick, *Amblyomma americanum*. *Infez. Med.* **2021**, *29*, 378–385. [[CrossRef](#)] [[PubMed](#)]
6. Sagurova, I.; Ludwig, A.; Ogden, N.H.; Pelcat, Y.; Dueymes, G.; Gachon, P. Predicted Northward Expansion of the Geographic Range of the Tick Vector *Amblyomma americanum* in North America under Future Climate Conditions. *Environ. Health Perspect.* **2019**, *127*, 107014. [[CrossRef](#)]
7. Tardy, O.; Acheson, E.S.; Bouchard, C.; Chamberland, É.; Fortin, A.; Ogden, N.H.; Leighton, P.A. Mechanistic movement models to predict geographic range expansions of ticks and tick-borne pathogens: Case studies with *Ixodes scapularis* and *Amblyomma americanum* in eastern North America. *Ticks Tick-Borne Dis.* **2023**, *14*, 102161. [[CrossRef](#)]
8. Koch, H.G. Suitability of White-Tailed Deer, Cattle, and Goats as Hosts for the Lone Star Tick, *Amblyomma americanum* (Acari: Ixodidae). *J. Kans. Entomol. Soc.* **1988**, *61*, 251–257.
9. Hofmeester, T.R.; Sprong, H.; Jansen, P.A.; Prins, H.H.T.; van Wieren, S.E. Deer presence rather than abundance determines the population density of the sheep tick, *Ixodes ricinus*, in Dutch forests. *Parasites Vectors* **2017**, *10*, 433. [[CrossRef](#)]
10. Larson, S.R.; Sabo, A.E.; Kruger, E.; Jones, P.; Paskewitz, S.M. *Ixodes scapularis* density in US temperate forests shaped by deer, earthworms, and disparate factors at two scales. *Ecosphere* **2022**, *13*, e3932. [[CrossRef](#)]
11. Bloemer, S.R.; Snoddy, E.L.; Cooney, J.C.; Fairbanks, K. Influence of Deer Exclusion on Populations of Lone Star Ticks and American Dog Ticks (Acari: Ixodidae). *J. Econ. Entomol.* **1986**, *79*, 679–683. [[CrossRef](#)]
12. Paddock, C.D.; Yabsley, M.J. Ecological havoc, the rise of white-tailed deer, and the emergence of *Amblyomma americanum*-associated zoonoses in the United States. *Curr. Top. Microbiol. Immunol.* **2007**, *315*, 289–324. [[CrossRef](#)] [[PubMed](#)]
13. Nair, A.D.; Cheng, C.; Jaworski, D.C.; Willard, L.H.; Sanderson, M.W.; Ganta, R.R. *Ehrlichia chaffeensis* infection in the reservoir host (white-tailed deer) and in an incidental host (dog) is impacted by its prior growth in macrophage and tick cell environments. *PLoS ONE* **2014**, *9*, e109056. [[CrossRef](#)]
14. Yabsley, M.J.; Varela, A.S.; Tate, C.M.; Dugan, V.G.; Stallknecht, D.E.; Little, S.E.; Davidson, W.R. *Ehrlichia ewingii* infection in white-tailed deer (*Odocoileus virginianus*). *Emerg. Infect. Dis.* **2002**, *8*, 668–671. [[CrossRef](#)] [[PubMed](#)]
15. Buller, R.S.; Arens, M.; Hmiel, S.P.; Paddock, C.D.; Sumner, J.W.; Rikhisa, Y.; Unver, A.; Gaudreault-Keener, M.; Manian, F.A.; Liddell, A.M.; et al. *Ehrlichia ewingii*, a newly recognized agent of human ehrlichiosis. *N. Engl. J. Med.* **1999**, *341*, 148–155. [[CrossRef](#)]
16. Tsao, J.I.; Hamer, S.A.; Han, S.; Sidge, J.L.; Hickling, G.J. The Contribution of Wildlife Hosts to the Rise of Ticks and Tick-Borne Diseases in North America. *J. Med. Entomol.* **2021**, *58*, 1565–1587. [[CrossRef](#)] [[PubMed](#)]
17. Williams, S.C.; Stafford, K.C.; Linske, M.A.; Brackney, D.E.; LaBonte, A.M.; Stuber, H.R.; Cozens, D.W. Effective control of the motile stages of *Amblyomma americanum* and reduced *Ehrlichia* spp. prevalence in adults via permethrin treatment of white-tailed deer in coastal Connecticut, USA. *Ticks Tick-Borne Dis.* **2021**, *12*, 101675. [[CrossRef](#)]
18. Wong, T.J.; Schramm, P.J.; Foster, E.; Hahn, M.B.; Schafrick, N.H.; Conlon, K.C.; Cameron, L. *The Effectiveness and Implementation of 4-Poster Deer Self-Treatment Devices for Tick-Borne Disease Prevention*; CDC: Atlanta, GA, USA, 2017; p. 32.
19. Nawrocki, C.C.; Piedmonte, N.; Niesobecki, S.A.; Rowe, A.; Hansen, A.P.; Kaufman, A.; Foster, E.; Meek, J.I.; Niccolai, L.; White, J.; et al. Acceptability of 4-poster deer treatment devices for community-wide tick control among residents of high Lyme disease incidence counties in Connecticut and New York, USA. *Ticks Tick-Borne Dis.* **2023**, *14*, 102231. [[CrossRef](#)]
20. Kaplan, Z.D.; Richardson, E.A.; Taylor, C.E.; Kaufman, P.E.; Weeks, E.N.I. Determination of the Discriminating Concentration Towards Permethrin for Surveying Resistance in *Amblyomma americanum*. *J. Med. Entomol.* **2022**, *59*, 922–929. [[CrossRef](#)]
21. Rosario-Cruz, R.; Domínguez-García, D.I.; Almazán, C. Inclusion of Anti-Tick Vaccines into an Integrated Tick Management Program in Mexico: A Public Policy Challenge. *Vaccines* **2024**, *12*, 403. [[CrossRef](#)]
22. Gonzalez, J.; Harvey, C.; Ribeiro-Silva, C.d.S.; Leal-Galvan, B.; Persinger, K.A.; Olafson, P.U.; Johnson, T.L.; Oliva Chavez, A. Evaluation of tick salivary and midgut extracellular vesicles as anti-tick vaccines in White-tailed deer (*Odocoileus virginianus*). *Ticks Tick-Borne Dis.* **2025**, *16*, 102420. [[CrossRef](#)]
23. Nawaz, M.; Malik, M.I.; Zhang, H.; Hassan, I.A.; Cao, J.; Zhou, Y.; Hameed, M.; Hussain Kuthu, Z.; Zhou, J. Proteomic Analysis of Exosome-Like Vesicles Isolated from Saliva of the Tick *Haemaphysalis longicornis*. *Front. Cell. Infect. Microbiol.* **2020**, *10*, 542319. [[CrossRef](#)]
24. Oliva Chávez, A.S.; Wang, X.; Marnin, L.; Archer, N.K.; Hammond, H.L.; Carroll, E.E.M.; Shaw, D.K.; Tully, B.G.; Buskirk, A.D.; Ford, S.L.; et al. Tick extracellular vesicles enable arthropod feeding and promote distinct outcomes of bacterial infection. *Nat. Commun.* **2021**, *12*, 3696. [[CrossRef](#)] [[PubMed](#)]
25. Xu, Z.; Wang, Y.; Sun, M.; Zhou, Y.; Cao, J.; Zhang, H.; Xuan, X.; Zhou, J. Proteomic analysis of extracellular vesicles from tick hemolymph and uptake of extracellular vesicles by salivary glands and ovary cells. *Parasit Vectors* **2023**, *16*, 125. [[CrossRef](#)]
26. Butler, L.R.; Singh, N.; Marnin, L.; Valencia, L.M.; O’Neal, A.J.; Paz, F.E.C.; Shaw, D.K.; Chavez, A.S.O.; Pedra, J.H.F. The role of Rab27 in tick extracellular vesicle biogenesis and pathogen infection. *Parasit Vectors* **2024**, *17*, 57. [[CrossRef](#)]
27. Mi, H.; Muruganujan, A.; Huang, X.; Ebert, D.; Mills, C.; Guo, X.; Thomas, P.D. Protocol Update for large-scale genome and gene function analysis with the PANTHER classification system (v.14.0). *Nat. Protoc.* **2019**, *14*, 703–721. [[CrossRef](#)]



28. Zhang, H.; Freitas, D.; Kim, H.S.; Fabijanic, K.; Li, Z.; Chen, H.; Mark, M.T.; Molina, H.; Martin, A.B.; Bojmar, L.; et al. Identification of distinct nanoparticles and subsets of extracellular vesicles by asymmetric flow field-flow fractionation. *Nat. Cell Biol.* **2018**, *20*, 332–343. [[CrossRef](#)] [[PubMed](#)]
29. Welsh, J.A.; Goberdhan, D.C.I.; O'Driscoll, L.; Buzas, E.I.; Blenkiron, C.; Bussolati, B.; Cai, H.; Di Vizio, D.; Driedonks, T.A.P.; Erdbrügger, U.; et al. Minimal information for studies of extracellular vesicles (MISEV2023): From basic to advanced approaches. *J. Extracell. Vesicles* **2024**, *13*, e12404. [[CrossRef](#)]
30. Perez-Riverol, Y.; Bai, J.; Bandla, C.; García-Seisdedos, D.; Hewapathirana, S.; Kamatchinathan, S.; Kundu, D.J.; Prakash, A.; Frericks-Zipper, A.; Eisenacher, M.; et al. The PRIDE database resources in 2022: A hub for mass spectrometry-based proteomics evidences. *Nucleic Acids Res.* **2022**, *50*, D543–D552. [[CrossRef](#)]
31. Li, J.; Smith, L.S.; Zhu, H.J. Data-independent acquisition (DIA): An emerging proteomics technology for analysis of drug-metabolizing enzymes and transporters. *Drug Discov. Today Technol.* **2021**, *39*, 49–56. [[CrossRef](#)]
32. Domingues, L.N.; Bendele, K.G.; Bodine, D.M.; Halos, L.; Cutolo, A.A.; Liebshtein, M.; Widener, J.; Figueiredo, M.; Moreno, Y.; Epe, C.; et al. A reverse vaccinology approach identified novel recombinant tick proteins with protective efficacy against *Rhipicephalus microplus* infestation. *Ticks Tick-Borne Dis.* **2024**, *15*, 102403. [[CrossRef](#)]
33. Rodríguez-Mallon, A. The Bm86 Discovery: A Revolution in the Development of Anti-Tick Vaccines. *Pathogens* **2023**, *12*, 231. [[CrossRef](#)] [[PubMed](#)]
34. Ndekezi, C.; Nkamwesiga, J.; Ochwo, S.; Kimuda, M.P.; Mwiine, F.N.; Tweyongyere, R.; Amanyire, W.; Muhanguzi, D. Identification of Ixodid Tick-Specific Aquaporin-1 Potential Anti-tick Vaccine Epitopes: An in-silico Analysis. *Front. Bioeng. Biotechnol.* **2019**, *7*, 236. [[CrossRef](#)]
35. Costa, G.C.A.; Ribeiro, I.C.T.; Melo-Junior, O.; Gontijo, N.F.; Sant'Anna, M.R.V.; Pereira, M.H.; Pessoa, G.C.D.; Koerich, L.B.; Oliveira, F.; Valenzuela, J.G.; et al. *Amblyomma sculptum* Salivary Protease Inhibitors as Potential Anti-Tick Vaccines. *Front. Immunol.* **2020**, *11*, 611104. [[CrossRef](#)]
36. Palmer, M.V.; Whipple, D.L.; Olsen, S.C.; Jacobson, R.H. Cell mediated and humoral immune responses of white-tailed deer experimentally infected with *Mycobacterium bovis*. *Res. Vet. Sci.* **2000**, *68*, 95–98. [[CrossRef](#)]
37. Waters, W.R.; Palmer, M.V.; Pesch, B.A.; Olsen, S.C.; Wannemuehler, M.J.; Whipple, D.L. MHC class II-restricted, CD4(+) T-cell proliferative responses of peripheral blood mononuclear cells from *Mycobacterium bovis*-infected white-tailed deer. *Vet. Immunol. Immunopathol.* **2000**, *76*, 215–229. [[CrossRef](#)] [[PubMed](#)]
38. Ditchkoff, S.S.; Lochmiller, R.L.; Masters, R.E.; Hooper, S.R.; Van Den Bussche, R.A. Major-histocompatibility-complex-associated variation in secondary sexual traits of white-tailed deer (*Odocoileus virginianus*): Evidence for good-genes advertisement. *Evolution* **2001**, *55*, 616–625. [[CrossRef](#)] [[PubMed](#)]
39. Ivy-Israel, N.M.D.; Moore, C.E.; Schwartz, T.S.; Ditchkoff, S.S. Characterization of two MHC II genes (DOB, DRB) in white-tailed deer (*Odocoileus virginianus*). *BMC Genet.* **2020**, *21*, 83. [[CrossRef](#)]
40. Parvizpour, S.; Pourseif, M.M.; Razmara, J.; Rafi, M.A.; Omid, Y. Epitope-based vaccine design: A comprehensive overview of bioinformatics approaches. *Drug Discov. Today* **2020**, *25*, 1034–1042. [[CrossRef](#)]
41. Paul, S.; Sidney, J.; Sette, A.; Peters, B. TepiTool: A Pipeline for Computational Prediction of T Cell Epitope Candidates. *Curr. Protoc. Immunol.* **2016**, *114*, 18.19.11–18.19.24. [[CrossRef](#)]
42. Kar, P.P.; Araveti, P.B.; Kuriakose, A.; Srivastava, A. Design of a multi-epitope protein as a subunit vaccine against lumpy skin disease using an immunoinformatics approach. *Sci. Rep.* **2022**, *12*, 19411. [[CrossRef](#)]
43. Knorr, S.; Reissert-Oppermann, S.; Tomás-Cortázar, J.; Barriales, D.; Azkargorta, M.; Iloro, I.; Elortza, F.; Pinecki-Socias, S.; Anguita, J.; Hovius, J.W.; et al. Identification and Characterization of Immunodominant Proteins from Tick Tissue Extracts Inducing a Protective Immune Response against *Ixodes ricinus* in Cattle. *Vaccines* **2021**, *9*, 636. [[CrossRef](#)] [[PubMed](#)]
44. Sharma, S.R.; Crispell, G.; Mohamed, A.; Cox, C.; Lange, J.; Choudhary, S.; Commings, S.P.; Karim, S. Alpha-Gal Syndrome: Involvement of *Amblyomma americanum*  $\alpha$ -D-Galactosidase and  $\beta$ -1,4 Galactosyltransferase Enzymes in  $\alpha$ -Gal Metabolism. *Front. Cell. Infect. Microbiol.* **2021**, *11*, 775371. [[CrossRef](#)]
45. Vechtova, P.; Sterbova, J.; Sterba, J.; Vancova, M.; Rego, R.O.M.; Selinger, M.; Strnad, M.; Golovchenko, M.; Rudenko, N.; Grubhoffer, L. A bite so sweet: The glycobiology interface of tick-host-pathogen interactions. *Parasit Vectors* **2018**, *11*, 594. [[CrossRef](#)] [[PubMed](#)]
46. Karim, S.; Leyva-Castillo, J.M.; Narasimhan, S. Tick salivary glycans—A sugar-coated tick bite. *Trends Parasitol.* **2023**, *39*, 1100–1113. [[CrossRef](#)] [[PubMed](#)]
47. Yoshikawa, S.; Miyake, K.; Kamiya, A.; Karasuyama, H. The role of basophils in acquired protective immunity to tick infestation. *Parasite Immunol.* **2021**, *43*, e12804. [[CrossRef](#)]
48. Arakane, Y.; Muthukrishnan, S. Insect chitinase and chitinase-like proteins. *Cell. Mol. Life Sci.* **2010**, *67*, 201–216. [[CrossRef](#)]
49. You, M.; Fujisaki, K. Vaccination effects of recombinant chitinase protein from the hard tick *Haemaphysalis longicornis* (Acari: Ixodidae). *J. Vet. Med. Sci.* **2009**, *71*, 709–712. [[CrossRef](#)]



50. Franta, Z.; Frantová, H.; Konvičková, J.; Horn, M.; Sojka, D.; Mareš, M.; Kopáček, P. Dynamics of digestive proteolytic system during blood feeding of the hard tick *Ixodes ricinus*. *Parasit Vectors* **2010**, *3*, 119. [CrossRef]
51. Lindenbergh, M.F.S.; Stoorvogel, W. Antigen Presentation by Extracellular Vesicles from Professional Antigen-Presenting Cells. *Annu. Rev. Immunol.* **2018**, *36*, 435–459. [CrossRef]
52. Ndawula, C., Jr.; Tabor, A.E. Cocktail Anti-Tick Vaccines: The Unforeseen Constraints and Approaches toward Enhanced Efficacies. *Vaccines* **2020**, *8*, 457. [CrossRef]
53. Luo, X.; McAndrews, K.M.; Arian, K.A.; Morse, S.J.; Boeker, V.; Kumbhar, S.V.; Hu, Y.; Mahadevan, K.K.; Church, K.A.; Chitta, S.; et al. Development of an engineered extracellular vesicles-based vaccine platform for combined delivery of mRNA and protein to induce functional immunity. *J. Control. Release* **2024**, *374*, 550–562. [CrossRef] [PubMed]
54. Chen, Y.; Douanne, N.; Wu, T.; Kaur, I.; Tsering, T.; Erzingatzian, A.; Nadeau, A.; Juncker, D.; Nerguizian, V.; Burnier, J.V. Leveraging nature's nanocarriers: Translating insights from extracellular vesicles to biomimetic synthetic vesicles for biomedical applications. *Sci. Adv.* **2025**, *11*, eads5249. [CrossRef] [PubMed]
55. Gai, C.; Pomatto, M.A.C.; Deregibus, M.C.; Dieci, M.; Piga, A.; Camussi, G. Edible Plant-Derived Extracellular Vesicles for Oral mRNA Vaccine Delivery. *Vaccines* **2024**, *12*, 200. [CrossRef]
56. Voordouw, M.J.; Tupper, H.; Önder, Ö.; Devevey, G.; Graves, C.J.; Kemps, B.D.; Brisson, D. Reductions in human Lyme disease risk due to the effects of oral vaccination on tick-to-mouse and mouse-to-tick transmission. *Vector-Borne Zoonotic Dis.* **2013**, *13*, 203–214. [CrossRef] [PubMed]
57. USDA-APHIS. Oral Rabies Vaccination. Available online: <https://www.aphis.usda.gov/national-wildlife-programs/rabies/vaccine> (accessed on 24 March 2025).

**Disclaimer/Publisher's Note:** The statements, opinions and data contained in all publications are solely those of the individual author(s) and contributor(s) and not of MDPI and/or the editor(s). MDPI and/or the editor(s) disclaim responsibility for any injury to people or property resulting from any ideas, methods, instructions or products referred to in the content.